

# Chemical Science

Volume 13  
Number 4  
28 January 2022  
Pages 851-1180

[rsc.li/chemical-science](https://rsc.li/chemical-science)




ISSN 2041-6539

Cite this: *Chem. Sci.*, 2022, 13, 934

All publication charges for this article have been paid for by the Royal Society of Chemistry

# Cracking the immune fingerprint of metal–organic frameworks†

T. Hidalgo, <sup>ab</sup> R. Simón-Vázquez, <sup>cd</sup> A. González-Fernández <sup>cd</sup>  
and P. Horcajada <sup>\*a</sup>

The human body is in a never-ending chess game against pathogens. When the immune system, our natural defence tool, is weakened, these organisms are able to escape, overcoming the body's contingency plan, which results in the body going into a pathological state. To overcome this checkmate status, emerging nanomedicines have been successfully employed as one of the best tactics for boosting the immune response, manipulating the body's defence tools for the specific recognition/elimination of pathological cells *via* the active ingredient delivery. However, the vast majority of these drug-delivery systems (DDS) are considered to be exclusively passive vehicles, with nanoscale metal–organic frameworks (nanoMOFs) attracting a great deal of attention due to their versatility and ability to carry and deliver exceptional drug payloads and to modulate their biological bypass. Nonetheless, their intrinsic immunogenicity character has been never addressed. Considering the immense possibilities that nanoMOFs offer as a treatment platform, the present study aimed to unveil the immunological fingerprint of MOFs, including an in-deep evaluation of the cellular oxidation balance, the inflammation and recruitment of immune cells and the precise Th1/Th2 cytokine profile that is triggered. This study aims to gain insights that will make more feasible the design of customized immune-active MOF nanoplatforms according to targeted diseases, as the next ace up immune system sleeve.

Received 27th July 2021  
Accepted 2nd November 2021

DOI: 10.1039/d1sc04112f

rsc.li/chemical-science

## Introduction

The use of immunotherapy to trigger the adequate cornerstones of the immune system is a recent tactic to treat challenging illnesses (*e.g.* cancer, infection, autoimmune diseases) as it allows manipulating the body's defence tools like in a game of chess. Through the immune system's machinery, the specific recognition/targeting or elimination of pathological tumoral cells along with refining the immunological memory are feasible.<sup>1,2</sup> While it is often associated with cancer, immunotherapy with monoclonal antibodies (mAbs) also serves as a benchmark to study other diseases (*e.g.* autoimmunity diseases, macular degeneration, allergies). Recently, the mAbs approach against immune-check point inhibitors was shown to offer real therapeutic success for many different cancer types. Moreover, cellular immunotherapy also offers appropriate responses, such as the adoptive therapies based on engineered

T cells (*e.g.* chimeric antibody receptor T (CAR-T) cells, natural killer (NK) cells, tumour infiltrating lymphocytes, dendritic cells). In some instances, the disease progression (*e.g.* metastasis, relapse or critical therapeutic failure) manages to escape from its constant surveillance, which makes it an arduous challenge to treat.<sup>3</sup> Thus, harnessing the immune response is a smart alternative to the current therapies (*i.e.* surgery, radiotherapy, chemotherapy).<sup>4,5</sup>

The clinical and preclinical treatment trends are not just limited to a single strategy as combined multiple treatments have demonstrated superior efficacy to any monotherapy. Thus, the combination of immunotherapy with other conventional treatment modalities can magnify the immune response, thereby maximizing their therapeutic effect. In this context, emerging nanomedicines have arisen as an appealing approach, as they are able to transport the desired active pharmaceutical ingredient (API, *e.g.* adjuvants, antigens, chemodrugs) in a safe and effective manner to the target cells and/or tissues.<sup>6</sup> However, the vast majority of such materials have been employed as passive vehicles, providing just API-protection against degradation and offering longer retention times in the body.<sup>7,8</sup> Revealing the NP inherent impact on the immune response (in absence of any APIs) would provide meaningful inputs for their *in vitro* and *in vivo* performance, allowing more personalized nanotherapies.<sup>2</sup>

<sup>a</sup>Advanced Porous Materials Unit (APMU), IMDEA Energy Institute, Av. Ramón de la Sagra 3, 28935 Móstoles-Madrid, Spain. E-mail: patricia.horcajada@imdea.org

<sup>b</sup>Institut Lavoisier, UMR CNRS 8180, Université de Versailles Saint-Quentin-en-Yvelines, 45 Av. des Etats-Unis, 78035 Versailles Cedex, France

<sup>c</sup>CINBIO, Immunology Group, Universidade de Vigo, 36310 Vigo, Spain

<sup>d</sup>Instituto de Investigación Sanitaria Galicia Sur (IIS Galicia Sur), SERGAS-UVIGO, Spain

† Electronic supplementary information (ESI) available. See DOI: 10.1039/d1sc04112f



Among the large variety of engineered nanocarriers (*e.g.* nanoparticles (NPs), liposomes, micelles), a new class of crystalline hybrid materials known as nanoscale metal–organic frameworks (nanoMOFs) has recently attracted a great deal of attention in the biomedical domain.<sup>9,10</sup> These hybrid NPs (composed of inorganic nodes and organic polydentate linkers assembled into multidimensional periodic lattices) can be precisely designed/manipulated at their molecular level, giving rise to multifunctional smart entities, which is known as *multifunctional efficiency*,<sup>11</sup> offering several advantages as drug-delivery systems (DDS), including: (i) chemical and structural versatility, which permits a suitable biocompatibility upon appropriate chemical design and the potential control of their *in vivo* fate; (ii) an ideal amphiphilic internal microenvironment, conveniently adapted to host a very broad variety of APIs (biological gases, cosmetics, enzymes, nucleic acids, drugs, *etc.*), releasing them in a controlled manner under physiological conditions; (iii) easy and scalable synthesis, following green methods with high yields; (iv) a general trend of a high biocompatible profile (*e.g.* the lack of *in vivo* toxicity for the benchmarked mesoporous Fe trimesate MIL-100(Fe) or the microporous Zr carboxylates Uio-66(Zr)); (v) additional abilities, where the recent successful external surface modification in some prototypes has proven the capability to endow further multifunctional abilities, such as targeting, imaging or enhanced stability (chemical/structural or colloidal) under biorelevant conditions.<sup>9,10,12–14</sup>

The latest advances on MOF nanocarriers have been mainly focused on their targeting *via* external functionalization and/or formulation.<sup>9,13</sup> However, their immunological impact has not been in the spotlight within the scientific community and still remains relatively unknown.

Most of the research reported so far on this topic is focused on cancer immunotherapy,<sup>3–5</sup> showing significant features exclusively when used as a passive vehicle for effectively releasing adjuvants, immunomodulators or antigens.<sup>15–18</sup> For instance, the first MOF-based vaccine using ZIF-8-loaded ovalbumin (OVA) with cytosine-phosphate-guanine oligodeoxynucleotide (CpG ODN) attached as an adjuvant prototype was able to activate a potent immune memory.<sup>19</sup> In terms of exploring the intrinsic immunogenicity behaviour of MOFs, some researchers have preliminarily evaluated the inflammatory response induced by iron-based MOFs modified on their surface with polymers.<sup>20,21</sup> However, despite the biomedical progress made over the last five years, the potential for MOFs to have intrinsically active repercussions at the immune level has not been investigated in depth. This basic notion is crucial, as it could provide valuable information about the innate features of MOFs and their precursors and their aroused immune reaction, which is a critical factor for boosting multi-therapy with diverse APIs.

Bearing this in mind, we decided to evaluate the immunogenicity of a selection of three different nanoMOF platforms: (i) two cubic-zeotype mesoporous metal ( $\text{Fe}^{3+}$  or  $\text{Al}^{3+}$ ) trimesates, namely MIL-100(Fe, Al) (MIL stands for the Material of the Institut Lavoisier) with a very important mesoporosity (surface area  $S_{\text{BET}} \sim 2400 \text{ m}^2 \text{ g}^{-1}$ , pore volume  $V_p \sim 1.2 \text{ cm}^3 \text{ g}^{-1}$ ),<sup>22</sup> which have been highlighted as efficient DDSs with a lack of *in vitro*

and *in vivo* toxicity;<sup>23</sup> and (ii) the cubic microporous zinc 2-methyl-imidazolite ZIF-8(Zn) (ZIF stands for zeolitic imidazolite framework), which can be described by a space-filling packing of a regular truncated octahedral ( $S_{\text{BET}} \sim 1800 \text{ m}^2 \text{ g}^{-1}$ ,  $V_p \sim 1.2 \text{ cm}^3 \text{ g}^{-1}$ ),<sup>24</sup> which has also been highly selected as a suitable MOF-based device for immunotherapy.<sup>17,18</sup> In all instances, we characterized their ability to induce human cytokine production and complementary activation, together with their potential cytotoxicity and production of reactive oxygen species (ROS).

Considering the immense possibilities that MOFs offer as a therapeutic platform (*e.g.* high porosity, versatile structure and biosafe character), shedding light on the specific roles of the MOFs and their constituents on the cellular homeostasis could tip the balance towards the generation of a therapeutic effect according to a targeted pathological dysfunction (*e.g.* cancer, infections, allergies, autoimmune diseases). In other words, MOFs could be used as potential immunoactivators or immunomodulatory carriers, able to induce immune activation or tolerance under a pathological or undesirable activation ('tunable immune response'). Therefore, unveiling the native MOF immunological fingerprint could provide insights to facilitate the design of a targeted immune-active MOF nano-platform for an efficient combined therapy.

## Results and discussion

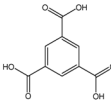
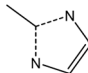
### NanoMOF characterization and biosafety profile

Despite the recent tendency to explore novel MOF applications in the biomedical field, where MOFs are mainly oriented as potential drug vehicles, the repercussion of their intrinsic impact on the immune system is still unknown. Since the physicochemical properties of nanocarriers highly impact their affinity to different biological structures (*e.g.* proteins, cells, tissues, nucleic acids), as well as their efficacy and/or bio-distribution (in other words, their biomedical performance),<sup>25,26</sup> we first fully characterized the nanoMOFs (XRPD, DLS, TEM, surface chemistry and colloidal stability, *etc.*; see Experimental section and the ESI,† for the synthetic and characterization details) prior to any immunological encounters.

The resulting materials displayed a nanometric particle size in aqueous solution (hydrodynamic diameter from DLS  $\sim 150$ , 220 and 110 nm for MIL-100(Al), MIL-100(Fe) and ZIF-8(Zn), respectively, see Table 1; which is in agreement with the microscopic observation acquired by TEM, see Fig. S1†), preserving in all cases their crystalline structure (Fig. S2†) and textural properties (Table 1), as previously reported.<sup>27,28</sup> However, it should be pointed out that there was a slight increase in the hydrodynamic diameter in the case of MIL-100(Al) compared to MIL-100(Fe), which could be related to an aggregation effect due to the proximity to more neutral  $\zeta$ -potential values (absence of enough electrostatic repulsions). This growth effect was also reflected in ZIF-8(Zn) NPs in comparison with a previously reported one (28 *vs.* 110 nm),<sup>24</sup> which was mainly associated with the nature of the medium used for its dispersion (EtOH *vs.* H<sub>2</sub>O, respectively), maintaining also their polydispersity index (PDI  $\sim 0.2$ ).



**Table 1** Particle size and  $\zeta$ -potential of MIL-100(Fe, Al) and ZIF-8 NPs in different physiological media together with their composition and specific surface area

	Media	MIL-100(Fe)	MIL-100(Al)	ZIF-8(Zn)
Composition	Metal	Fe	Al	Zn
	Ligand			
Size (nm) (PdI)	H <sub>2</sub> O	153 ± 53(0.3)	218 ± 28(0.2)	110 ± 48(0.2)
	PBS	177 ± 17(>0.3)	209 ± 41(>0.3)	227 ± 26(>0.3)
	RPMI	145 ± 38(0.3)	248 ± 50(>0.3)	284 ± 22(>0.3)
$\zeta$ -Potential (mV)	H <sub>2</sub> O	-25 ± 4	-7 ± 3	+96 ± 0
	PBS	-32 ± 0	-16 ± 1	-27 ± 1
	RPMI	-31 ± 2	-10 ± 2	-9 ± 2
BET surface (m <sup>2</sup> g <sup>-1</sup> ) <sup>a</sup>	1530	1510	1400	

<sup>a</sup> Brunauer–Emmett–Teller (BET) surface area.

Regarding the above-mentioned  $\zeta$ -potential outcomes, the fluctuation of the nanoMOF surface charge observed here should be related to the diverse proportions of the partially coordinated cations *vs.* the linkers when exposed to the physiological media. For instance, the more negative  $\zeta$ -potential values displayed by MIL-100(Fe) NPs compared to their aluminium analogue (-25 ± 4 *vs.* -7 ± 3 mV, respectively, Table 1) could be due to the higher amount of carboxylate/carboxylic acid *vs.* cation and/or the presence of elements on the surface of Fe-F (fluorine coming from a washing step in the MIL-100(Fe) preparation). Similarly, despite the contrary  $\zeta$ -potential value obtained on the external ZIF-8(Zn) surface, the high positive charge (+96 ± 0 mV) could be explained by the same trend: a large proportion of cations or a higher presence of protonated ligands, as the pH of the aqueous solution was lower than the pK<sub>a</sub> of the imidazolite (6.0 *vs.* 7.0 and 14.9).<sup>29,30</sup>

Bearing in mind the high-impact of the surrounding media on the NP stability, and hence, on their biological affinities, biodistribution and efficacy,<sup>25,26</sup> the nanoMOF particle size and  $\zeta$ -potential were investigated under diverse simulated physiological conditions: from a simple phosphate buffer solution (PBS) to a more complex medium consisting of supplemented cell culture media (RPMI, Table 1). In all cases, the nanometric range was maintained, exhibiting an average size close to 160 and 225, and 207 nm for MIL-100(Fe & Al) and ZIF-8 NPs, respectively. However, the ZIF-8(Zn) NPs underwent a notable size increase in the presence of more complex media (from 110 ± 48 nm in H<sub>2</sub>O to 227 ± 26 or 284 ± 22 nm in PBS or RPMI, respectively, Table 1). This destabilizing effect was related to the tremendous  $\zeta$ -potential fluctuation, shifting from a highly positive charge in H<sub>2</sub>O to a lower negative character in PBS and RPMI (+96 ± 0 *vs.* -27 ± 1 and -9 ± 2 mV, respectively). This dramatic conversion has been already observed in other nanoMOF prototypes due to the formation of a superficial corona composed by phosphate groups and/or other salts/proteins from the media.<sup>20,27</sup> Overall, the colloidal stability of the tested nanoMOFs in these biorelevant media makes them suitable candidates for the assessment of their immunological recognition.

Prior to exploring the associated immune fingerprint of these nanoMOFs and their future implications, their toxicological character needed also to be evaluated. On this basis, a macrophage cell line (J774.A1) was selected as an appropriate model of the first defence line in the immune system against pathogens (those involved in the *innate* immune response).<sup>31,32</sup> Remarkably, an absence of toxicity was observed by the MTT method<sup>33</sup> for both MIL-100 (Fe & Al) and ZIF-8(Zn) NPs after 24 h incubation even at very high concentrations (1.2 mg mL<sup>-1</sup>, Fig. S3†). Despite previous data suggesting a higher cytotoxicity tendency induced by ZIF-8(Zn) than MIL-100(Fe) NPs (maybe as a consequence of a potential competition between Zn<sup>2+</sup> *vs.* Fe<sup>2+</sup> *vs.* Ca<sup>2+</sup> through ion channels and/or deoxyribonucleic acid (DNA) damage),<sup>28,34</sup> as well as the often associated cytotoxicity effect of diverse cationic carriers,<sup>35</sup> these outcomes were in good agreement with the lack of severe toxicity observed in other cell lines<sup>9,21,34</sup> as well as with previous *in vivo* data.<sup>10,12</sup> Therefore, the biofriendly profile obtained from these nanoMOFs could enable further investigations into their self-immunoactive activity. In other words, shedding light on the interaction between MOFs and/or its precursors with the immune constituents could support the generation of a specific therapeutic activity, providing valuable data starting from their particular affinities with the biological surrounding, type of internalization pathways according to the cellular source and their influence on specific chemical reactions, such as catalytic and oxidative processes. Thus, in the next section, the MOF recognition by essential actors of the innate immune system is addressed considering (i) the cellular oxidation balance *via* reactive oxidative stress production (ROS), (ii) the complementary activation and (iii) the cytokine secretion pattern.

### NanoMOF immune fingerprint: innate and adaptive immunity

**Innate immunity: chess opening.** The exogenous intervention of engineered nanomaterials into the human body entails their participation in the modulation of cellular redox homeostasis; where a moderate concentration of ROS can act as a second messenger for physiological regulation (activating the



immune system), while excessive ROS may overwhelm the antioxidant cell capacity, generating cellular toxicity, and consequently, triggering cell death. Thus, understanding the nanoMOF impact on the cellular redox status could guide the therapeutic effect to a specific pathological dysfunction (*e.g.* cancer, infections, allergies, autoimmune diseases).<sup>36</sup> It has been reported that the immune recognition of metal/metal oxide NPs could be associated not only with potential nanotoxicity (due to the metal leaching, increasing the ROS production), but also to a positive immunogenicity role of the released ions.<sup>37,38</sup>

Given that we are proposing three nanoMOFs based on different cations ( $\text{Fe}^{3+}$ ,  $\text{Al}^{3+}$  and  $\text{Zn}^{2+}$ ), their repercussion on the cellular oxidation balance should be investigated. To address this point, a human promyelocytic leukaemia cell line (HL-60) was selected, as it has been shown to modulate ROS production in a dose-dependent response.<sup>21,39</sup> Two different doses (25 and  $250 \mu\text{g mL}^{-1}$ ) of MIL-100(Fe, Al) and ZIF-8(Zn) NPs were put in contact with the HL-60 cells at different time points (1, 4, 8 and 24 h), and the results compared with three different controls: (i) a positive control (C+), cells incubated with PMA (ROS inducer); (ii) the basal control ( $C_{\text{basal}}$ ), the intrinsic oxidation state of HL-60 cells (in the absence of ROS inducer but with the ROS reactant) and (iii) a negative control (C-), cells in media without any treatment (neither the ROS inducer or the ROS reactant; see the Experimental section). Remarkably, no ROS induction was detected at short times ( $\leq 8$  h) regardless of the NPs' concentration, with the exception of the highest concentration of MIL-100(Al) NPs ( $250 \mu\text{g mL}^{-1}$ ), which exhibited a slight increase in oxidative stress (Fig. 1). On the contrary, at longer incubation times (24 h), ROS production rose in all cases at high dose ( $250 \mu\text{g mL}^{-1}$ ), being more prominent in the MIL-100(Al) NPs (even at the lowest concentration). This oxidative stress, promoted by the Al-trimesate, was higher than with its Fe-analogue or Zn based NPs, displaying an oxidative strength tendency of  $\text{Al} > \text{Fe} \sim \text{Zn}$ . Therefore, all the tested nanoMOFs induced moderate ROS at 24 h, being stronger for the MIL-100(Al) NPs; this performance could be beneficial to enhancing their potential immunotherapeutic effect as the immune system can be smoothly activated ('friendly warning'), as previously proposed for other nanoparticle systems.<sup>29,38</sup> In fact, it is not the first occasion that ROS production by innate immune cells has been related to a good *in vivo* adjuvancy, as an immune activation mechanism is triggered.<sup>40</sup>

Consequently, the nature of the metal seems to be a crucial parameter as the redox homeostasis could be tampered with.<sup>36,41</sup> Although the mechanism is not well-described, these metals favour superoxide radical formation [mainly the superoxide anion ( $\text{O}_2^{\cdot-}$ ), hydrogen peroxide ( $\text{H}_2\text{O}_2$ ), singlet oxygen ( $^1\text{O}_2$ ) and hydroxyl radical ( $\cdot\text{OH}$ )].<sup>36</sup> In our particular case, despite the non-redox character of Al compounds, MIL-100(Al) NPs have proven to be a powerful *in vitro* and *in vivo* pro-oxidant,<sup>42,43</sup> promoting both iron auto-oxidation and ROS formation by their binding with superoxide radical anions.<sup>44,45</sup> Most of the  $\text{Al}^{3+}$  present in the human organism is not free in solution, but forms stable complexes with low/high molecular mass biomolecules, with around 90% of the aluminium in the

blood serum bounded to the transferrin protein.<sup>46</sup> Concerning  $\text{Fe}^{3+}$ , it is widely reported that iron oxides (*e.g.*  $\text{Fe}_3\text{O}_4$ ,  $\text{Fe}_2\text{O}_3$ ) can induce ROS production through the Fenton reaction (catalyzing the  $\text{H}_2\text{O}_2$  reaction), showing high reactivity with biological molecules such as lipids, proteins and DNA.<sup>47,48</sup> In fact, iron is generally bound to specific proteins, leaving few free iron cations available for the Fenton reaction (*e.g.* inducing ferroptosis).<sup>49</sup> In our particular case, the moderate ROS levels of MIL-100(Fe) NPs were also in agreement with an increase in the *in vitro*<sup>34</sup> and *in vivo*<sup>12</sup> oxidative stress, as already previously described by some of us, demonstrating a totally reversible effect after 2 weeks of its intravenous administration with a high dose (up to  $220 \text{ mg kg}^{-1}$ ). Finally, the redox-inert  $\text{Zn}^{2+}$  is the most abundant metal in the brain, being also an essential component in various enzymes and transcription factors involved in the regulation of key cellular functions (DNA replication, repair of DNA damage, cell cycle progression and apoptosis).<sup>41</sup> The depletion of zinc may enhance DNA damage by impairing DNA repair mechanisms, generating free radicals: its high solubility and easy nitrogen- or oxygen-coordination lead to the formation of chelates with many biomolecules that are involved in the oxidative balance homeostasis, resulting in their inactivation and then, the induction of ROS.<sup>50</sup> For instance,  $\text{Zn}^{2+}$  is associated with the inhibition of the important antioxidant enzyme glutathione reductase.<sup>51,52</sup> Besides, zinc competition with other redox active metals (such as copper or iron) may also play a role in oxidative stress-mediated damage, as  $\text{Zn}^{2+}$  may bind and protect sulfhydryl groups belonging to proteins. In contrast, other researchers have also proposed a possible antioxidant and anti-inflammatory effect of this cation associated with (i) potential activation of the antioxidant enzyme superoxide dismutase (SOD1 and 3), which possesses Zn and Cu in its active metal site and (ii) inhibition of the nicotinamide adenine dinucleotide phosphate (NADPH) oxidase, which involved in free radical production.<sup>53,54</sup>

Therefore, the moderate oxidative stress generated by ZIF-8(Zn) NPs would favour designing a dual functionality (oxidant and antioxidant behaviour) according to the immune system demand. In other words, the presence of additional metals and the potential action of the selected nanoMOFs will be determined by the particular cellular status and/or pathological environment to be treated. Thus, previous knowledge of each clinical condition would lead to more precise nanoMOF therapies.

#### Innate immunity tour: the pivotal point in the middle game.

On the other hand, apart from the above-mentioned activation of innate immune cells during a pathogen invasion (*e.g.* macrophages, natural killers-NK cells, innate lymphoid cells), humoral factors are also triggered. This is the case of the complement system, a complex network of plasma proteins that can elicit highly efficient and tightly regulated inflammatory and cytolytic immune responses to infectious organisms, tissue damage by physical, chemical, or neoplastic insults, and other surfaces identified as 'non-self'.<sup>37,55</sup> It has been proven that the contact with nanomaterials can activate this system through three pathways (classical, lectin or alternative), leading to particle opsonization and clearance.<sup>56</sup> Typically, the



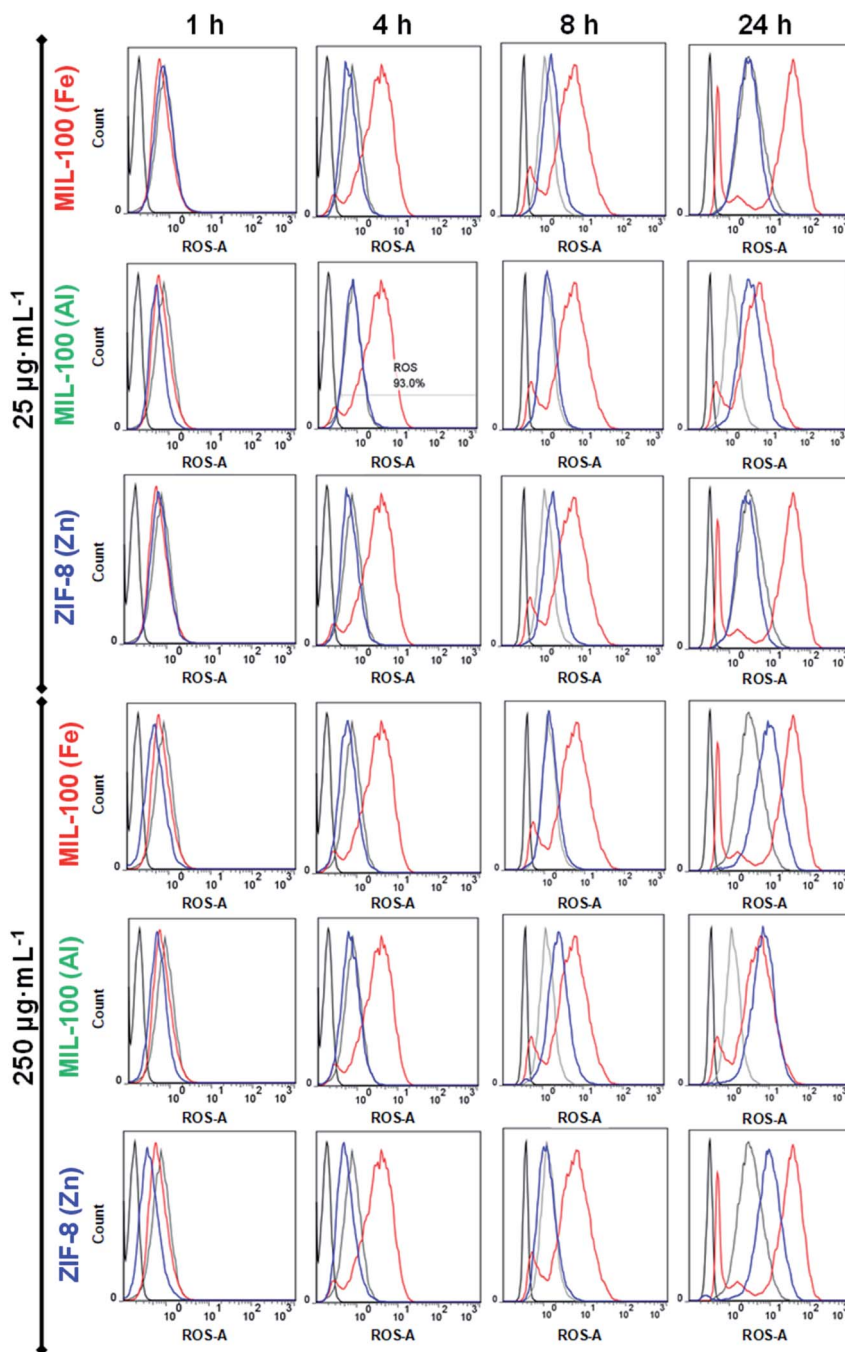


Fig. 1 ROS production in HL60 cells incubated with MIL-100(Fe) (top), MIL-100(Al) (middle) and ZIF-8(Zn) NPs (bottom) at two different concentrations (25 and 250  $\mu\text{g mL}^{-1}$ ; marked with a blue line). Basal (cells), negative (cells + ROS reagent) and positive control (cells + ROS reagent + ROS inducer) are disclosed in black, grey and red lines, respectively. Note that these data, corresponding to one of the triplicates obtained in four independent experiments ( $n = 12$ ), are totally representative from the whole results.

degradation of the central factor C3 promotes the membrane attack complex (MAC) to create pores in the lipid bilayers (thereby accelerating tissue damage and inflammation) as well as the production of anaphylatoxins, which behave as inflammatory alert signals attracting immune cells to the zone.<sup>57</sup> In this context, the ability of nanoMOFs to mediate the complement pathway and, in turn, the inflammation process and recruitment of immune cells were investigated. A pool of

human sera from three different donors were put in contact with two different concentrations (25 and 250  $\mu\text{g mL}^{-1}$ ) of MIL-100(Fe, Al) and ZIF-8(Zn) NPs, using western blotting to evaluate the degradation of the common factor C3, a protein that fulfils a pivotal role in the three complement cascades (see Experimental section). Overall, there was no induction of the complement cascades at high concentration (250  $\mu\text{g mL}^{-1}$ ), regardless of the MOF nature. Nonetheless, it should be noted



that both MIL-100(Al) and ZIF-8(Zn) NPs slightly stimulated this system at low concentration ( $25 \mu\text{g mL}^{-1}$ ; Fig. 2), with the effect being even higher in the case of MIL-100(Al) NPs. The ROS and complementary activation (both relevant adjuvant mechanisms) observed with these nanoMOFs were in agreement with the induction effect of alum, the first and most widely used adjuvant in vaccines.<sup>58</sup> Hence, these findings make them potentially attractive as good adjuvants, with potential for heading to the next level of immune surveillance, *i.e.* activation of the adaptive immunity, which could be combined with specific antigens.

**Adaptive immunity tour: best tactics for the endgame.** As stated, this recognition by the innate immune system (*e.g.* macrophage recognition or activation of the complement cascade) is a critical point; diverse parameters can stimulate

this response in different sensing pathways, which can be designed to determine the class of infecting pathogens (based on their localization, viability, replication or virulence) and to be translated into signals (extracellular factors: cytokines –CK–) that, together with the antigen presentation to T cells, will contribute to initiating an appropriate specific adaptive immune response. Note, a suitable adjuvant/vaccine task is generally expected to elicit a specific and long-term immune response,<sup>59,60</sup> keeping active the specific immune memory (T & B cells, long-live plasma cells) with the main aim of maintaining the ‘immune warning status = checkmate’ until the pathological battle is over.

Moreover, a lack of inflammatory signals or the presence of regulatory factors during antigen presentation can promote tolerogenic responses, suppressing immune reactions (*e.g.*

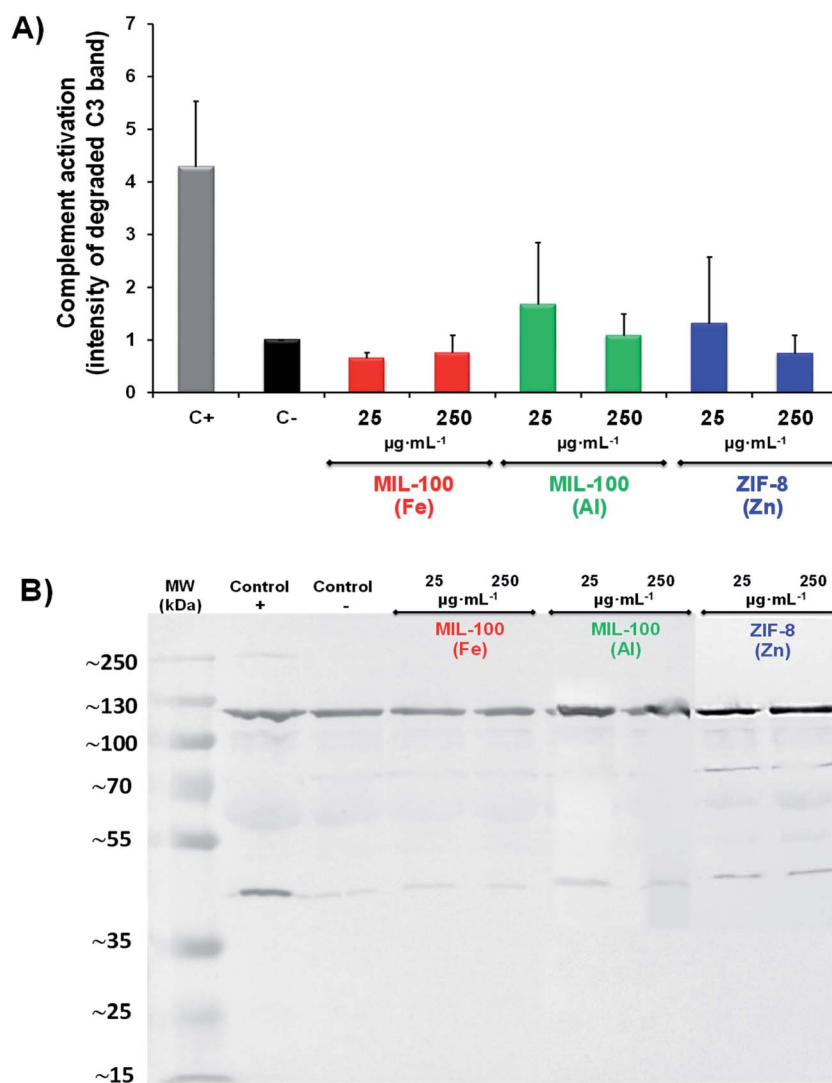


**Fig. 2** Top: Complement activation, represented by determining the intensity of the band at 43 kD, corresponding to the degraded C3 factor, and compared with the band at 115 kD, corresponding to the intact protein. The samples were normalized with respect to the negative control. Bottom: Complement activation data for MIL-100(Fe), MIL-100 (Al) and ZIF-8 (Zn) NPs determined by western blotting (WB) using a specific C3 antibody to measure the degradation of the protein. Note that these data correspond to one example of the duplicates obtained in three independent experiments ( $n = 6$ , 3 different WB experiments), totally representative of the whole results, and the error bars correspond to the standard deviation. All data were tested by one-way ANOVA test ( $p < 0.05$  was considered statistically significant).



Table 2 Summary of the cytokine production<sup>a</sup>

		NPs dose ( $\mu\text{g mL}^{-1}$ )	Positive control (LPS & PHA)	MIL-100 (Fe)	MIL-100 (Al)	ZIF-8 (Zn)
Th1 cytokines	IL-12p70	25	3/3	3/3	2/3	3/3
		250	( $10^2$ to $10^3$ )	( $10^2$ to $10^3$ )	(10 to $10^2$ )	(10 to $10^2$ )
	INF- $\gamma$	25	3/3	2/3	3/3	2/3
		250	( $10^3$ to $10^4$ )	( $10^2$ to $10^3$ )	(10 to $10^2$ )	(10 to $10^2$ )
	IL-2	25	2/3	2/3	2/3	3/3
		250	( $10^2$ to $10^3$ )	(10 to $10^2$ )	(10 to $10^2$ )	(10 to $10^2$ )
Anti-inflammatory cytokine	IL-10	25	2/3	2/3	2/3	2/3
		250	( $10^3$ to $10^4$ )	( $10^3$ to $10^4$ )	( $10^3$ to $10^4$ )	( $10^2$ to $10^3$ )
Pro-inflammatory cytokines	IL-6	25	3/3	3/3	3/3	2/3
		250	(> $10^5$ )	( $10^2$ to $10^3$ )	(> $10^5$ )	(> $10^5$ )
	IL-8	25	2/3	2/3	2/3	3/3
		250	( $10^3$ to $10^4$ )	( $10^2$ to $10^3$ )	( $10^3$ to $10^4$ )	( $10^3$ to $10^4$ )
	IL-1 $\beta$	25	3/3	3/3	3/3	2/3
		250	( $10^2$ to $10^3$ )	( $10^3$ to $10^4$ )	( $10^3$ to $10^4$ )	( $10^3$ to $10^4$ )
	TNF- $\alpha$	25	3/3	2/3	3/3	2/3
		250	( $10^3$ to $10^4$ )	(> $10^5$ )	( $10^4$ to $10^5$ )	( $10^4$ to $10^5$ )
TNF- $\beta$	25	3/3	2/3	3/3	2/3	
	250	( $10^3$ to $10^4$ )	( $10^2$ to $10^3$ )	(10 to $10^2$ )	(10 to $10^2$ )	

<sup>a</sup> Secretion of Th2 cytokines (IL-4 and IL-5) was not observed with the MIL-100(Fe), MIL-100(Al) and ZIF-8 (Zn) NPs. The values correspond to the variation of the cytokines concentration (in  $\text{pg mL}^{-1}$ ) compared with the negative control (10,  $10^2$ ,  $10^3$ ,  $10^4$  or  $>10^5$  times) obtained from 3 different donors (1/3, 2/3 or 3/3), with the representation of the activation shown in the positive control (LPS and PHA, which acted as inducers of the cytokines production).

modulating inflammation, restricting migration of self-reactive immune cells),<sup>64</sup> which could be a great scenario for combined immuno- and chemo-therapeutic nanocarriers for autoimmune and allergic diseases, among others.

The transition from innate to adaptive immunity requires antigen processing and T cell presentation by antigen-presenting cells (APCs): dendritic cells (DC) are able to trigger naïve T cells that, with the already activated macrophages and B cells (effectors of the antibody production), can promote the activation of helper T cells (CD4<sup>+</sup>), which is crucial for a specific immune response and immunological memory.<sup>5,6</sup>

However, it should be mentioned that the immunological scenario and its consequent action rely on the type of disease. For instance, (i) in a tumoral environment, a high presence of immunocompromised cells is observed, where the therapeutic approach aims to reverse this immunosuppression by stimulating the immune system; or (ii) when facing viral pathogens (e.g. SARS-Cov-2), the current vaccine treatments aim to induce both B and T cell responses, either by the generation of neutralizing antibodies or anti-viral specific helper and/or

cytotoxic T cells (CD8<sup>+</sup>) as well as long-live memory cells;<sup>62</sup> (iii) on the contrary, for the autoreactivity and inflammatory processes concerned with autoimmune and autoinflammatory diseases, the induction of a tolerance response is required. Consequently, revealing the intrinsic immunogenicity of nanomaterials can be exploited to modulate the immune response; whereby understanding the molecular action mechanisms of different cytokines in the context of a specific disease could contribute to developing more targeted anti-cytokine/cytokine therapy ('innovative nanotherapeutic immunomodulating strategies').<sup>6</sup>

To shed light on the type of adaptive immune response elicited by the nanoMOF, and thereby its potential role as a therapeutic carrier of diverse diseases, two different concentrations (25 and 250  $\mu\text{g mL}^{-1}$ ) were incubated with human peripheral blood mononuclear cells (PBMCs) from three voluntary donors (see Experimental section; Table 2) for the determination of their cytokine profile. It should be noted that the PBMC fraction was mainly composed of lymphocytes (70–90% including T, B and NK cells) and monocytes (10–30%), generally activated in





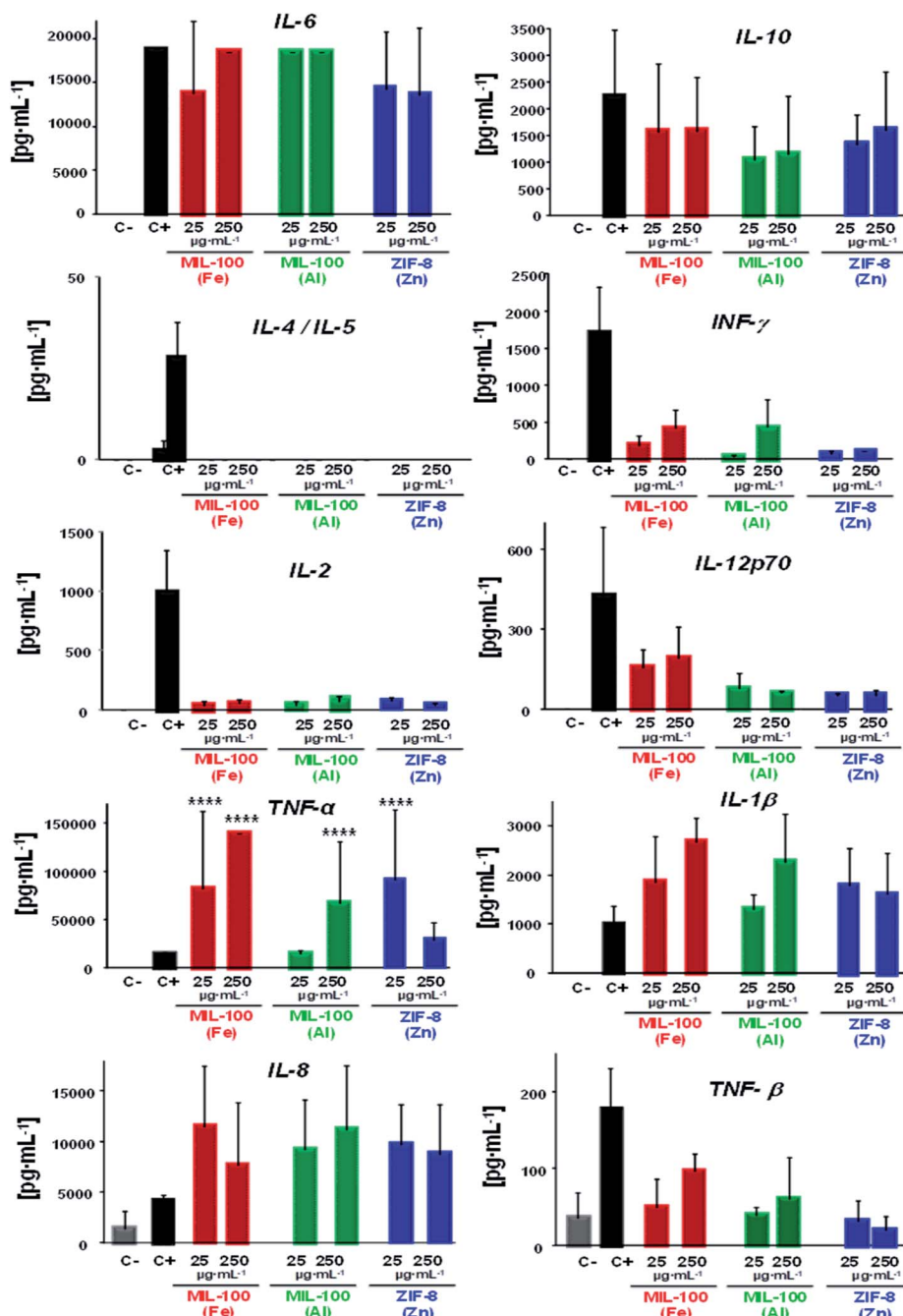


Fig. 3 Individual levels of human cytokines production from peripheral blood mononuclear cells (3 different donors) after 24 h in contact with 25 or 250  $\mu\text{g mL}^{-1}$  of MIL-100(Fe), MIL-100(Al) or ZIF-8(Zn) NPs. C-: negative control (PBS) and C+: positive control (10  $\mu\text{g mL}^{-1}$  PHA + 1  $\text{mg mL}^{-1}$  LPS). All data were tested by two-way ANOVA and Tukey's tests ( $P < 0.05$  was considered statistically significant).

response to external stimuli, such as the nanoMOFs or positive controls (selected here as C+: lipopolysaccharide –LPS– and lectin phytohemagglutinin –PHA–), which are also known as human cytokine activators. In particular, the cytokine profile was here represented as the average of three donors' values for each nanoMOF in comparison with the negative control (C-) together with the number of donors included within this variation (Table 2), for greater clarity.

On the whole, a substantial immune response was evidenced in presence of the three nanoMOFs; whereby a diverse cytokine

production 10 to  $>10^5$  times higher than the negative control was obtained (see Table 2; Fig. 3), highlighting a general secretion of pro-inflammatory cytokines in all cases (mostly derived from the activated monocytes). One example was IL-6, secreted by the activated monocytes, which participate in diverse functions, such as the B cell growth or endocrine effects (e.g. induction of fever, production of reactive C protein in the liver). In this case, similar values were obtained for the positive control, being more than  $10^5$  times higher than the negative control. Other significant pro-inflammatory cytokines observed



here were interleukin IL-1 $\beta$  (relevant cytokine for the activation of T and B lymphocytes) along with the tumour necrosis factor (TNF,  $\alpha$  and  $\beta$  responsible for the signalling pathways for cell survival, apoptosis, inflammatory responses or cellular differentiation), displaying levels higher than for C $^-$ , from  $10^3$  to  $10^4$  for IL-1 $\beta$  and  $\sim 10^4$  to  $>10^5$  in the case of TNF $\alpha$  (being even 10 to  $10^2$  times higher than for C $^+$  in both cases), which suggest that the tested nanoMOFs significantly induced inflammation. On the contrary, high levels of the anti-inflammatory IL-10 were also observed within the same range than for the positive control with  $\sim 10^3$  to  $10^4$  times higher values than for the negative control. Although they can be produced by different cell types, such as Th2 cells or regulatory T and B cells, activated monocytes are also able to be secreted in large amounts.

However, this secretion is usually delayed in the presence of other pro-inflammatory factors, as shown here with the IL-6, tumour necrosis factor or INF- $\gamma$  production (the main Th1 cytokine implicated in the inflammation and proliferation of the macrophages). Regarding the chemokine IL-8, which is a potent chemoattracting agent, its levels were also raised with values  $\sim 10^3$  to  $10^4$  higher than cells incubated with the media containing MIL-100(Al) and ZIF-8(Zn) NPs, being 10 times lower in the case of MIL-100(Fe) NPs. These findings reveal a great trend of those nanoMOFs to be recognized by the innate cells.

An expected optimal scenario should include a well-balanced Th1 and Th2 response, as this would be suited to a particular immune challenge. In view of unveiling the potential type of adaptive immune response induced by these nanoMOFs, the specific influence pursued by Th1–Th2 cytokines was investigated in depth. Related with Th1 stimulation, the interplay of interleukin 2 (IL-2, involved in T and NK cells proliferation), interferon gamma (IFN $\gamma$ ) and Th2 cytokine profiles (IL-4 and IL-5, which are the main markers of Th2 cells, promoting specific cellular differentiation) showed low levels of IL-2 regardless of the nature of the MOF (Table 2, Fig. 3), with levels slightly higher for those of IFN $\gamma$  with MIL-100(Fe) and (Al) than with ZIF-8(Zn) NPs. In both cases, the levels produced by these Th1 cells were 10 to  $10^2$  times higher than those in the negative control. Similar to IL-2, IL12p70 production in the presence of MIL-100(Al) and ZIF-8(Zn) NPs was  $\sim 10$  to  $10^2$  times higher than in cells incubated with the media, with the exception of MIL-100(Fe) NPs, where the values reached the positive control levels. It should be noted that this last interleukin stimulates the Th1 profile and inhibits the Th2 response.<sup>63</sup> In fact, looking deeper into the Th2 cell impact, no secretion of IL-4 or IL-5 were detected notwithstanding the MOF topology or composition. These outputs evidence the activation of mainly the cellular response vs. the humoral (antibody), which can be beneficial for vaccine purposes, for instance.<sup>57</sup>

Overall, all the nanoMOFs seemed to be very well-recognized by the innate monocyte population, eliciting a potent response with the secretion of pro-inflammatory cytokines together with the chemokine IL-8. Conversely, IL-10 release, produced by activated monocytes and other immune cells after exposure to nanoMOFs, could indicate the tendency of the cells to revert to this pro-inflammatory status, showing higher IL-10 levels that might be also associated with a slight INF- $\gamma$  inhibition. This CK pattern, detected on human cells, reflects the type of immune

response that one could expect if these nanoMOFs were to be used *in vivo*.

In a nutshell, the lack of IL-4 and IL-5 (the main markers of the Th2 profile), the presence of IL-2, IL12p70 and IFN $\gamma$  (distinctive Th1 profile) and the induction of IL-6, IL1 $\beta$  and TNF $\alpha$  (involved in inflammatory processes) suggest that the presence of nanoMOFs could tip the balance to the Th1 responses (highly recommended for anti-tumoral, anti-viral and/or intracellular bacteria responses), promoting their specific differentiation.

## Conclusions

Understanding the native immunological features of nanoMOFs could make it possible to customize the design of effective nanomedicines to prevent and/or treat specific pathological disorders. Each nanoMOF has a unique biological repercussion: their large versatility (type of metal/linker nature, topology, reactivity, *etc.*) requires specific safety profiles, considering not only the cellular but also the geno and/or immunological impact.

The nanoMOFs studied here (*i.e.* MIL-100(Al), MIL-100(Fe) and ZIF-8(Zn)) showed a high biocompatible profile with a slight activation of the complement cascade along with ROS induction in innate cells, especially for the innate monocytes, displaying the production of both several pro-inflammatory (IL-6, TNF $\alpha$  and  $\beta$ , IL1 $\beta$ , IL-8) and anti-inflammatory (IL-10) cytokines. Despite all showing a very similar pattern, MIL-100(Fe) seemed to induce a higher Th1 immune response compared to MIL-100(Al) and ZIF-8(Zn) NPs, with a higher induction of INF- $\gamma$  and IL12p70 cytokines. Moreover, the lack of Th2 response elicited by any nanoMOF was noteworthy, which could suggest a slight cellular response (antibody production).

Overall, the activation of innate and Th1 cells induced by these nanoMOFs make them promising adjuvant candidates for targeted immunotherapy. These findings should help to create more novel and effective immunoactive MOFs, opening new horizons not only in biomedicine (*e.g.* therapy, imaging, vaccines) but also in other economically and societally relevant fields, such as the environment, catalysis or sensing, in which the safety of the MOFs is a crucial parameter to their practical use.

## Author contributions

TH and PH: synthesis, characterisation cellular toxicity; TH, RSV, AGF, and PH: immunological studies (ROS, Complement, CKs). The manuscript was written through contributions of all authors. All authors have given approval to the final version of the manuscript.

## Conflicts of interest

There are no conflicts to declare.

## Acknowledgements

This work was partially supported by the Labex NanoSaclay financial support for the MSc studies (ANR-11-IDEX-0003-02)



together with the CNRS, IMDEA Energy and Xunta de Galicia (GRC-ED431C 2020/02) funding. T. H. and P. H. acknowledge the Regional Madrid Founding (Talento 2018 Modality 2, (2018-T2/IND-11407), the Multifunctional Metalloodrugs in Diagnosis and Therapy Network (MICIU, RED2018-102471-T) and the European Union's Horizon 2020 Research and Innovation Programme under the Marie Skłodowska-Curie grant agreement No 897678. P. H. acknowledges the Spanish Ramón y Cajal Programme (grant agreement no. 2014 to 16823).

## References

- X. Zhong and X. Sun, *Acta Pharmacol. Sin.*, 2020, **41**, 928.
- W. Sang, Z. Zhang, Y. Dai and X. Chen, *Chem. Soc. Rev.*, 2019, **48**, 3771.
- L. Scheetz, K. S. Park, Q. Li, P. R. Lowenstein, M. G. Castro, A. S. Schwendeman and J. J. Moon, *Nat. Biomed. Eng.*, 2019, **3**, 768.
- N. Papaioannou, O. V. Beniata, P. Vitsos, O. Tsitsilonis and P. Samara, *Ann. Transl. Med.*, 2016, **4**, 261.
- M. L. Guevara, F. Persano and S. Persano, *Semin. Cancer Biol.*, 2021, **69**, 238–348.
- K. Naran, T. Nundalall, S. Chetty and S. Barth, *Front. Microbiol.*, 2018, **9**, 3158.
- C. T. Perciani, L. Y. Lui, L. Wood and S. A. MacParland, *ACS Nano*, 2021, **15**, 7.
- C. D'Amico, F. Fontana, R. Cheng and H. A. Santos, *Drug Deliv. Transl. Res.*, 2021, **11**, 353.
- J. Yang and Y. W. Yang, *Small*, 2020, **16**, 1906846.
- S. Rojas, A. Arenas-Vivo and P. Horcajada, *Coord. Chem. Rev.*, 2019, **388**, 202.
- R. Freund, U. Lächelt, T. Gruber, B. Rühle and S. Wuttke, *ACS Nano*, 2018, **12**, 2094.
- P. Horcajada, T. Chalati, C. Serre, B. Gillet, C. Sebrie, T. Baati, J. F. Eubank, D. Heurtaux, P. Clayette, C. Kreuz, J. S. Chang, Y. K. Hwang, V. Marsaud, P. B. Bories, L. Cynober, S. Gil, G. Férey, P. Couvreur and R. Gref, *Nat. Mater.*, 2010, **9**, 172.
- S. Wuttke, M. Lismont, A. Escudero, B. Rungtaweeworant and W. J. Parak, *Biomaterials*, 2017, **123**, 172.
- S. Yuan, L. Feng, K. Wang, J. Pang, M. Bosh, C. Lollar, Y. Sun, J. Qin, X. Yang, P. Zhang, Q. Wang, L. Zou, Y. Zhang, L. Zhang, Y. Fang, J. Li and H. C. Zhou, *Adv. Mater.*, 2018, **30**, 1704303.
- Y. B. Miao, W. Y. Pan, K. H. Chen, H. J. Wei, F. L. Mi, M. Y. Lu, Y. Chang and H. W. Sung, *Adv. Funct. Mater.*, 2019, **29**(43), 1904828.
- X. F. Zhong, Y. T. Zhang, L. Tan, T. Zheng, Y. Y. Hou, X. Y. Hong, G. Du, X. Chen, Y. Zhang and X. Sun, *J. Control. Release*, 2019, **300**, 81.
- Y. Yang, Q. Chen, J. P. Wu, T. B. Kirk, J. Xu, Z. Liu and W. Xue, *ACS Appl. Mater. Interfaces*, 2018, **10**, 12463.
- H. Zhang, J. Zhang, Q. Li, A. Song, H. Tian, J. Wang, Z. Li and Y. Luan, *Biomaterials*, 2020, **245**, 119983.
- Y. Zhang, F. M. Wang, E. G. Ju, Z. Liu, Z. W. Chen, J. S. Ren and X. Qu, *Adv. Funct. Mater.*, 2016, **26**, 6454.
- E. Bellido, T. Hidalgo, M. V. Lozano, M. Guillevic, R. Simón-Vázquez, M. J. Santander-Ortega, Á. González-Fernández, C. Serre, M. J. Alonso and P. Horcajada, *Adv. Healthc. Mater.*, 2015, **4**, 1246.
- T. Hidalgo, M. Giménez-Marqués, E. Bellido, J. Avila, M. C. Asensio, F. Salles, M. V. Lozano, M. Guillevic, R. Simón-Vázquez, Á. González-Fernández, C. Serre, M. J. Alonso and P. Horcajada, *Sci. Rep.*, 2017, **7**, 43099.
- A. García-Márquez, A. Demessence, A. E. Platero-Prats, D. Heurtaux, P. Horcajada, C. Serre, J. S. Chang, G. Férey, V. A. Peña-O'Shea, C. Boissière, D. Grosso and C. Sanchez, *Eur. J. Inorg. Chem.*, 2012, **32**, 5165.
- M. Giménez-Marqués, T. Hidalgo and P. Horcajada, *Coord. Chem. Rev.*, 2016, **307**, 342.
- J. Cravillon, S. Munzer, S. J. Lohmeier, A. Feldhoff, K. Huber and M. Wiebcke, *Chem. Mater.*, 2009, **21**, 1410.
- S. Mitragotri, P. A. Burkre and R. Langer, *Nat. Rev. Drug Discovery*, 2014, **13**, 650.
- E. Fattal and N. Tsapis, *Clin. Transl. Imaging*, 2014, **2**, 77.
- E. Bellido, M. Guillevic, T. Hidalgo, M. J. Santander-Ortega, C. Serre and P. Horcajada, *Langmuir*, 2014, **30**, 5911.
- R. Grall, T. Hidalgo, J. Delic, A. Garcia-Marquez, S. Chevillarda and P. Horcajada, *J. Mater. Chem. B*, 2015, **3**, 8279.
- A. Phan, C. J. Doonan, F. J. Uribe-Romo, C. B. Knobler, M. O'Keeffe and O. M. Yaghi, *Acc. Chem. Res.*, 2010, **43**, 58.
- S. Luo, P. G. Wang and J. P. Cheng, *J. Org. Chem.*, 2004, **69**, 555.
- L. Franken, M. Schiwon and C. Kurts, *Cell. Microbiol.*, 2016, **18**, 475.
- D. Hirayama, T. Iida and H. Nakase, *Int. J. Mol. Sci.*, 2018, **19**, 92.
- S. Arora, J. R. Rajwade and K. M. Paknikar, *Toxicol. Appl. Pharmacol.*, 2012, **258**, 151.
- C. Tamames-Tabar, D. Cunha, E. Imbuluzqueta, F. Ragon, C. Serre, M. J. Blanco-Prieto and P. Horcajada, *J. Mater. Chem. B*, 2014, **2**, 262.
- C. Teijeiro, A. McGlone, N. Csaba, M. Garcia-Fuentes and M. J. Alonso, *Handbook of Nanobiomedical Research*, World Scientific Ed., 2014.
- B. Yang, Y. Chen and J. Shi, *Chem. Rev.*, 2019, **119**, 4881.
- B. Fadeel, *Front. Immunol.*, 2019, **133**, 1.
- V. Mallikarjun, D. J. Clarke and C. J. Campbell, *Free Radic. Biol. Med.*, 2012, **53**, 280.
- M. D. Ferrer, A. Sureda, A. Mestre, J. A. Tur and A. Pons, *Cell. Physiol. Biochem.*, 2010, **25**, 241.
- M. Peleteiro, E. Presas, J. V. González-Aramundiz, B. Sánchez-Correa, R. Simón-Vázquez, N. Csaba, M. J. Alonso and A. González-Fernández, *Front. Immunol.*, 2018, **9**, 791.
- M. Valko, K. Jomova, C. J. Rhodes, K. Kuča and K. Musilek, *Arch. Toxicol.*, 2016, **90**, 1.
- C. Exley, *Free Radic. Biol. Med.*, 2004, **36**, 380.
- J. I. Mujika, F. Ruipérez, I. Infante, J. M. Ugalde, C. Exley and X. Lopez, *J. Phys. Chem. A*, 2011, **115**, 6717.
- C. Exley, P. Siesjo and H. Eriksson, *Cell Press*, 2010, **31**, 103.



- 45 F. Ruipérez, J. Mujika, J. Ugalde, C. Exley and X. Lopez, *J. Inorg. Biochem.*, 2012, **117**, 118.
- 46 J. Mujika, G. Dalla Torre and X. Lopez, *Phys. Chem. Chem. Phys.*, 2018, **20**, 16256.
- 47 H. J. H. Fenton, *J. Chem. Soc. Trans.*, 1894, **65**, 899.
- 48 M. Wlaschek, K. Singh, A. Sindrilaru, D. Crisan and K. Scharffetter-Kochanek, *Free Radic. Biol. Med.*, 2019, **133**, 262.
- 49 X. Qiana, J. Zhang, Z. Gud and Y. Chenc, *Biomaterials*, 2019, **211**, 1.
- 50 Y. Chang, M. Zhang, L. Xia, J. Zhang and G. Xing, *Materials*, 2012, **5**, 2850.
- 51 M. G. Bishop, R. Dringen and S. R. Robinson, *Free Radic. Biol. Med.*, 2007, **42**, 1222.
- 52 R. Ryu, Y. Shin, J. W. Choi, W. Min, H. Ryu, C. R. Choi and H. Ko, *Exp. Brain Res.*, 2002, **143**, 257.
- 53 A. S. Prasad, *Curr. Opin. Clin. Nutr.*, 2009, **12**, 646.
- 54 Y. Song, S. W. Leonard, M. G. Traber and E. Ho, *J. Nutr.*, 2009, **139**, 1626.
- 55 M. G. Netea, A. Schlitzer, K. Placek, L. A. B. Joosten and J. L. Schultze, *Cell Host Microbe*, 2019, **25**, 13.
- 56 M. A. Dobrovolskaia and S. E. McNeil, *Handbook of Immunological properties of Engineered Nanomaterials*, World Scientific Publishing Co. Inc., 2012.
- 57 J. Szebeni, D. Simberg, Á. González-Fernández, Y. Barenholz and M. A. Dobrovolskaia, *Nat. Nanotechnol.*, 2018, **13**, 1100.
- 58 T. R. Ghimire, *SpringerPlus*, 2015, **4**, 181.
- 59 R. S. Oakes, E. Froimchuk and C. M. Jewell, *Adv. Ther.*, 2019, **2**, 1800150.
- 60 A. Iwasaki and R. Medzhitov, *Nat. Immunol.*, 2015, **16**, 343.
- 61 J. M. Gammon and C. M. Jewell, *Adv. Healthc. Mater.*, 2019, **8**, 1801401.
- 62 G. Canedo-Marroquín, F. Saavedra, C. A. Andrade, R. V. Berrios, L. Rodríguez-Guilarte, M. C. Opazo, C. Riedel and A. M. Kalergis, *Front. Immunol.*, 2020, **11**, 569760.
- 63 M. Elsabahy and K. L. Wooley, *Chem. Soc. Rev.*, 2013, **42**, 5552.

